

Analysis of Bonding and d-Electron Count in the Transition-Metal Carbides and Transition-Metal-Silicide Carbides with Discrete Linear M–C–M Units (M = Cr, Fe, Re) by Electronic Structure Calculations

H.-J. Koo and M.-H. Whangbo*

Department of Chemistry, North Carolina State University, Raleigh, North Carolina 27695-8204

Received November 12, 1998

Electronic structures of the silicide carbides $\text{Tm}_2\text{Fe}_2\text{Si}_2\text{C}$, $\text{Th}_2\text{Re}_2\text{Si}_2\text{C}$, and ThFe_2SiC and the carbide $\text{Ho}_2\text{Cr}_2\text{C}_3$ were calculated, using the extended Hückel tight binding method, to probe the d-electron counts of their transition metal atoms M (Cr, Fe, Re) the bonding of their linear M–C–M (M = Cr, Fe, Re) units. The nature of the short interlayer $\text{X}\cdots\text{X}$ (X = C, Si) bonds in $\text{Tm}_2\text{Fe}_2\text{Si}_2\text{C}$, $\text{Th}_2\text{Re}_2\text{Si}_2\text{C}$, and $\text{Ho}_2\text{Cr}_2\text{C}_3$ was also examined. Our study shows that the M–C bonds of the M–C–M units exist as double bonds. There is significant bonding in the interlayer $\text{Si}\cdots\text{Si}$ contacts of the silicide carbides $\text{R}_2\text{M}_2\text{Si}_2\text{C}$ (M = Fe, Re). The transition-metal atoms exist as d^{10} ions in $\text{Tm}_2\text{Fe}_2\text{Si}_2\text{C}$ and $\text{Th}_2\text{Re}_2\text{Si}_2\text{C}$. The d-electron count is slightly lower than d^{10} in ThFe_2SiC and close to d^5 in $\text{Ho}_2\text{Cr}_2\text{C}_3$.

Introduction

The structural motif of the transition-metal carbides $\text{R}_2\text{Cr}_2\text{C}_3$ (R = Y, Gd–Lu)^{1–3} is similar to that of the transition-metal silicide carbides $\text{R}_2\text{Fe}_2\text{Si}_2\text{C}$ (R = La, Ce, Nd, Sm, Tb, Dy, Tm, Lu, Th)^{4–7} and $\text{R}_2\text{Re}_2\text{Si}_2\text{C}$ (R = Y, La–Nd, Gd–Er, Th).⁷ These compounds contain discrete linear M–C–M (M = Cr, Fe, Re) units, so that their formulas can be written as $\text{R}_2(\text{MCM})\text{X}_2$ (M = Cr, X = C; M = Fe, Re, X = Si). Linear M–C–M units are also found in the silicide carbides RFe_2SiC (R = Y, Sm, Gd, Tb–Tm, Lu, Th, U),^{8,9} and their formulas can be written as $\text{R}(\text{MCM})\text{X}$ (M = Fe, X = Si). These $\text{R}(\text{MCM})\text{X}$ and $\text{R}_2(\text{MCM})\text{X}_2$ phases share other common structural features as well (see below). Jeitschko and co-workers showed that neither the Cr atoms of the carbides $\text{R}_2\text{Cr}_2\text{C}_3$ nor the Fe atoms of the silicide carbides $\text{R}_2\text{Fe}_2\text{Si}_2\text{C}$ ⁶ carry magnetic moments.¹ This implies that the 3d orbitals of Cr and Fe overlap strongly with the s/p orbitals of their ligand atoms and/or that all the d-block levels are filled completely. In support of the first possibility, the linear M–C–M units of these compounds are found to possess short M–C bonds.^{1,6,7} Thus, Jeitschko and co-workers treated the M–C bonds of $\text{R}_2\text{M}_2\text{Si}_2\text{C}$ (M = Fe, Re) as double bonds in their electron counting in terms of the 18-electron rule. The Fe–C bonds of the silicide carbides RFe_2SiC are almost as short as those of the silicide carbides $\text{R}_2\text{Fe}_2\text{Si}_2\text{C}$ (e.g., 1.842 Å in ThFe_2SiC ⁶ and 1.802 Å in $\text{Tm}_2\text{Fe}_2\text{Si}_2\text{C}$ ⁸), and

the Cr–C bonds of $\text{R}_2\text{Cr}_2\text{C}_3$ are also short (e.g., 1.906 Å in $\text{Ho}_2\text{Cr}_2\text{C}_3$).¹ The $\text{R}_2\text{M}_2\text{X}_2\text{C}$ compounds (M = Cr, X = C; M = Fe, Re, X = Si) contain layers of composition $\text{M}_2\text{X}_2\text{C}$. The $\text{M}_2\text{Si}_2\text{C}$ layers of the silicide carbides $\text{R}_2\text{M}_2\text{Si}_2\text{C}$ (M = Fe, Re) make short interlayer $\text{Si}\cdots\text{Si}$ contacts. They are slightly longer than the Si–Si bond (2.35 Å) in elemental silicon⁹ (e.g., 2.592 Å in $\text{Tm}_2\text{Fe}_2\text{Si}_2\text{C}$,⁶ 2.660 Å in $\text{Dy}_2\text{Fe}_2\text{Si}_2\text{C}$,⁴ and 2.741 Å in $\text{Th}_2\text{Re}_2\text{Si}_2\text{C}$ ⁷) but much shorter than the van der Waals distance (4.20 Å)¹⁰ between two silicon atoms. In the $\text{R}_2\text{Cr}_2\text{C}_3$ systems, however, the shortest C···C distance (3.604 Å) between the adjacent Cr_2C_3 layers is longer than the van der Waals distance (3.40 Å)¹⁰ between two carbon atoms.

To understand why the M–C bonds of the RM_2SiC and $\text{R}_2\text{M}_2\text{X}_2\text{C}$ compounds are short, it is necessary to examine the nature of bonding in their M–C–M units. For the $\text{R}_2\text{M}_2\text{X}_2\text{C}$ systems, it is interesting to investigate why the interlayer $\text{Si}\cdots\text{Si}$ contacts are shorter than the van der Waals distance, while this is not the case for the interlayer C···C contacts. Our recent studies^{11,12} showed that the Si 3p orbitals of the phosphosilicides MSi_mP_n (M = Cu, Ni, Pt, Co, Rh, Ir, Fe)^{13–18} act as acceptor orbitals to the transition-metal d-orbitals and hence make the d-electron count of their transition-metal atoms close to d^{10} (Herein, the term “acceptor orbital” is used from the viewpoint of orbital interaction between filled and empty levels, for which the empty orbital that stabilizes the filled orbital lying below is referred to as the acceptor orbital.¹⁹) Thus, it is

* To whom correspondence should be addressed.

- (1) Jeitschko, W.; Behrens, R. K., *Z. Metallkd.* **1986**, *77*, 788.
- (2) Zeppenfeld, K.; Pöttgen, R.; Reehuis, M.; Jeitschko, W.; Behrens, R. K. *J. Phys. Chem. Solids* **1993**, *54*, 257.
- (3) Reehuis, M.; Zeppenfeld, K.; Jeitschko, W.; Ressouche, E. *J. Alloys Compd.* **1994**, *209*, 217.
- (4) Paccard, L.; Paccard, D. *J. Less-Common Met.* **1988**, *136*, 297.
- (5) Le Roy, J.; Paccard, D.; Bertrand, C.; Soubeyroux, J. L.; Bouillot, J.; Paccard, L.; Schmitt, D. *Solid State Commun.* **1993**, *86*, 675.
- (6) Pöttgen, R.; Ebel, T.; Evers, C. B. H.; Jeitschko, W. *J. Solid State Chem.* **1995**, *114*, 66.
- (7) Hüfken, T.; Witte, A. M.; Jeitschko, W. *J. Alloys Compd.* **1998**, *266*, 158.
- (8) Witte, A. M.; Jeitschko, W. *J. Solid State Chem.* **1994**, *112*, 232.
- (9) Donohue, J. *The Structures of the Elements*; Wiley: New York, 1974.

- (10) Bondi, A. *J. Phys. Chem.* **1964**, *68*, 441.
- (11) Lee, K.-S.; Koo, H.-J.; Dai, D.; Ren, J.; Whangbo, M.-H. *Inorg. Chem.* **1999**, *38*, 340.
- (12) Lee, K.-S.; Koo, H.-J.; Ren, J.; Whangbo, M.-H. *J. Solid State Chem.*, in press.
- (13) Perrier, Ch.; Kirschen, M.; Vincent, H.; Gottlieb, U.; Chenevier, B.; Madar, R. *J. Solid State Chem.* **1997**, *133*, 473.
- (14) Wallinda, J.; Jeitschko, W. *J. Solid State Chem.* **1995**, *114*, 476.
- (15) Kaiser, P.; Jeitschko, W. *Z. Anorg. Allg. Chem.* **1996**, *622*, 53.
- (16) Kirschen, M.; Vincent, H.; Perrier, Ch.; Chaudouât, P.; Chenevier, B.; Madar, R. *Mater. Res. Bull.* **1995**, *30*, 507.
- (17) Vincent, H.; Kreisel, J.; Perrier, Ch.; Chaix-Pluchery, O.; Chaudouât, P.; Madar, R. *J. Solid State Chem.* **1996**, *124*, 366.
- (18) Perrier, Ch.; Vincent, H.; Chaudouât, P.; Chenevier, P.; Madar, R. *Mater. Res. Bull.* **1995**, *30*, 357.

Table 1. Exponents z_i and Valence Shell Ionization Potentials H_{ii} of Slater-Type Orbitals c_i Used for Extended Hückel Tight-Binding Calculation^a

atom	χ_i	H_{ii} (eV)	ζ_i	c_1^b	ζ_i'	c_2^b
Cr	4s	-8.66	1.772	1.0		
Cr	4p	-5.24	1.400	1.0		
Cr	3d	-11.2	5.410	0.3830	2.340	0.7367
Fe	4s	-9.10	1.925	1.0		
Fe	4p	-5.32	1.390	1.0		
Fe	3d	-12.6	6.068	0.4038	2.618	0.7198
Re	6s	-9.36	2.346	1.0		
Re	6p	-5.96	1.730	1.0		
Re	5d	-12.7	4.340	0.5886	2.309	0.5627
C	2s	-19.2	1.608	1.0		
C	2p	-11.8	1.568	1.0		
Si	3s	-14.7	1.634	1.0		
Si	3p	-8.08	1.428	1.0		

^a H_{ii} 's are the diagonal matrix elements $\langle \chi_i | H^{eff} | \chi_i \rangle$, where H^{eff} is the effective Hamiltonian. In our calculations of the off-diagonal matrix elements $H^{eff} = \langle \chi_i | H^{eff} | \chi_j \rangle$, the weighted formula was used. See: Ammeter, J.; Bürgi, H.-B.; Thibault, J.; Hoffmann, R. *J. Am. Chem. Soc.* **1978**, *100*, 3686. ^b Contraction coefficients used in the double- ζ Slater-type orbital.

important to see if this is true for the silicide carbides RFe_2SiC and $R_2M_2Si_2C$ ($M = Fe, Re$). If so, the Fe atoms of these compounds would not carry magnetic moments. In the present work, we probed these questions by calculating the electronic structures of $Tm_2Fe_2Si_2C$, $Th_2Re_2Si_2C$, $Ho_2Cr_2C_3$, and $ThFe_2SiC$ based on the extended Hückel tight binding method.²⁰ The parameters of the atomic orbitals employed in our calculations are summarized in Table 1.²¹

Crystal Structures of $R_2M_2X_2C$ and RM_2XC

To facilitate our description of the electronic structures of $R_2M_2X_2C$ and RM_2XC , it is necessary to consider their crystal structures briefly. Each transition metal atom M is located at a tetrahedral site made up of one C and three X atoms (Figure 1a). Each X atom is located at a tetrahedral site made up of one X and three M atoms such that the M and X atoms form a double-tetrahedral chain, as depicted in Figure 1b, where the $X \cdots X$ and $M-C$ bonds are omitted for simplicity. A projection view of this double-tetrahedral chain along the chain direction (i.e., the crystallographic b -axis direction) can be represented as shown in Figure 1c. Then, the M_2X_2C framework of $R_2M_2X_2C$ results when the double-tetrahedral chains are linked together by the $M-C-M$ and $X \cdots X$ bonds as shown in Figure 2a. The M_2XC framework of RM_2XC results when the double-tetrahedral chains share the X atoms and are linked by the $M-C-M$ bonds as depicted in Figure 2b. In the M_2X_2C and M_2XC frameworks, every four adjacent double-tetrahedral chains form a channel running along the chain direction, and the R atoms are accommodated in these channels.

Molecular Orbitals of the Linear $M-C-M$ Units

Figure 3 shows the bottom 14 molecular orbital (MO) levels calculated for the $M-C-M$ units found in $Tm_2Fe_2Si_2C$,

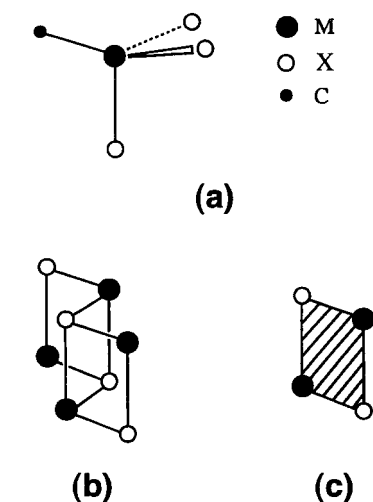


Figure 1. Structural building blocks of $R_2M_2X_2C$ ($M = Fe, Re, X = Si$; $M = Cr, X = C$) and RM_2XC ($M = Fe, X = Si$). (a) Tetrahedral arrangement around the transition-metal M. (b) Perspective view of a double-tetrahedral chain made up of C, M, and X atoms. For simplicity, the $M-C$ and $X \cdots X$ bonds are omitted (see Figure 2). (c) Projection view of the double-tetrahedral chain along the chain direction.

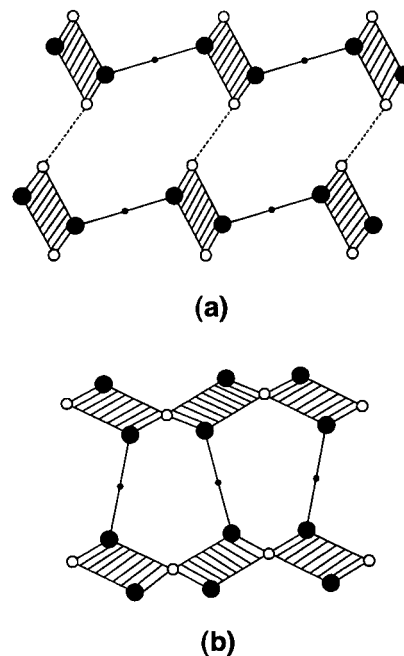


Figure 2. Projection views of (a) the M_2X_2C of $R_2M_2X_2C$ and (b) the M_2XC framework of RM_2XC along the direction of the double-tetrahedral chain.

$Th_2Re_2Si_2C$, $ThFe_2SiC$, and $Ho_2Cr_2C_3$. These levels are grouped into four s, three p, and two d levels, where the p and d levels are each doubly degenerate. The nodal properties of the s, p, and d levels are presented in parts a–c of Figure 4, respectively. The main contributor to the s_1 level is the C 2s orbital, and the C 2s level lies well below the C 2p and the transition metal nd levels. Thus, the s_1 level is well-separated from the remaining 13 levels. The pattern of the top 13 MO levels is similar in $Tm_2Fe_2Si_2C$ and $ThFe_2SiC$ (Figure 3) because their $Fe-C-Fe$ units have similar $Fe-C$ bond lengths. The top 13 levels of the $Re-C-Re$ unit are spread in a wider energy region compared with those of the $Fe-C-Fe$ units (Figure 3b). In the $Cr-C-Cr$ unit, the top 10 MO levels occur in a narrow energy region and are well-separated from the three levels lying below (Figure 3d).

(19) Albright, T. A.; Burdett, J. K.; Whangbo, M.-H. In *Orbital Interactions in Chemistry*, Wiley: New York, 1985.

(20) (a) Whangbo, M.-H.; Hoffmann, R. *J. Am. Chem. Soc.* **1978**, *100*, 6397. (b) Our calculations were performed using the CAESAR program package (Ren, J.; Liang, W.; Whangbo, M.-H., 1998. For details, see: <http://www.PrimeC.com/>).

(21) The atomic orbital energies determined by Clementi and Roetti from Hartree-Fock calculations were used to have a balanced set of H_{ii} values. See: Clementi, E.; Roetti, C. *Atomic Data Nuclear Data Tables* **1974**, *14*, 177.

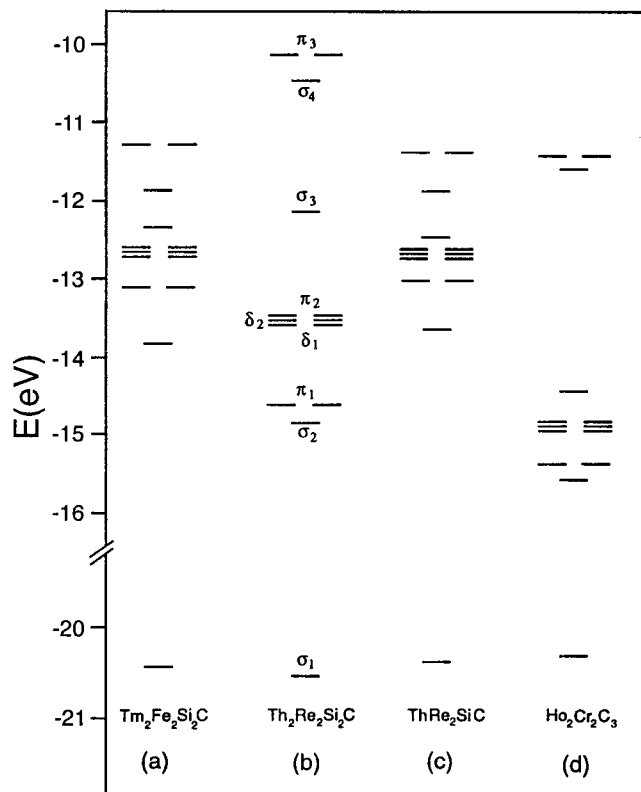


Figure 3. 14 low-lying molecular orbital levels calculated for the linear M–C–M units of (a) $\text{Tm}_2\text{Fe}_2\text{Si}_2\text{C}$, (b) $\text{Th}_2\text{Re}_2\text{Si}_2\text{C}$, (c) ThFe_2SiC , and (d) $\text{Ho}_2\text{Cr}_2\text{C}_3$.

The σ_1 , σ_2 , and π_1 orbitals (see Figure 4a–c) are bonding and the δ_1 , δ_2 , and π_2 orbitals are nonbonding in the M–C bond regions. Therefore, the M–C bond becomes a double bond when the four bonding MOs are each doubly filled. This double bond character is maintained until all the six nonbonding MOs are each doubly filled. The σ_3 , σ_4 , and π_3 levels would be antibonding in the M–C bond regions were it not for the contributions of the $(n + 1)$ s/p orbitals of M. The latter atomic orbitals hybridize the M *nd* orbitals to reduce antibonding in the M–C bonds. Table 2 summarizes how the overlap populations of the M–C bonds change as the number of the valence electrons *N* on the M–C–M unit increases from 20 to 22 to 24 to 28. With $N = 20$, the four bonding and the six nonbonding levels of M–C–M are doubly filled. With $N = 22$, 24, and 28, the σ_3 , σ_4 , and π_3 levels of M–C–M become doubly filled. The M–C overlap population is nearly unchanged when the σ_3 level is filled and increases somewhat when the σ_4 level is filled. As the π_3 level is filled, the overlap population is reduced essentially to the value found for $N = 20$. This means that the M–C bond of the M–C–M unit should be considered as a double bond even when all the σ_3 , σ_4 , and π_3 levels are completely filled. In the latter case, one may regard the M–C–M unit as consisting of three closed-shell anions, i.e., one C^{4-} and two d^{10} metal ions. Nevertheless, the M–C bonds remain strongly bound from the effect of the $(n + 1)$ s/p orbitals of M. In discrete organometallic compounds, the $\text{Cr}=\text{C}$, $\text{Fe}=\text{C}$ and $\text{Re}=\text{C}$, double bonds are in the 1.91–2.05, 1.68–1.79, and 1.87–2.05 Å range, respectively.²² These values are in support of our assignment that the M–C bond of the M–C–M unit is a double bond.

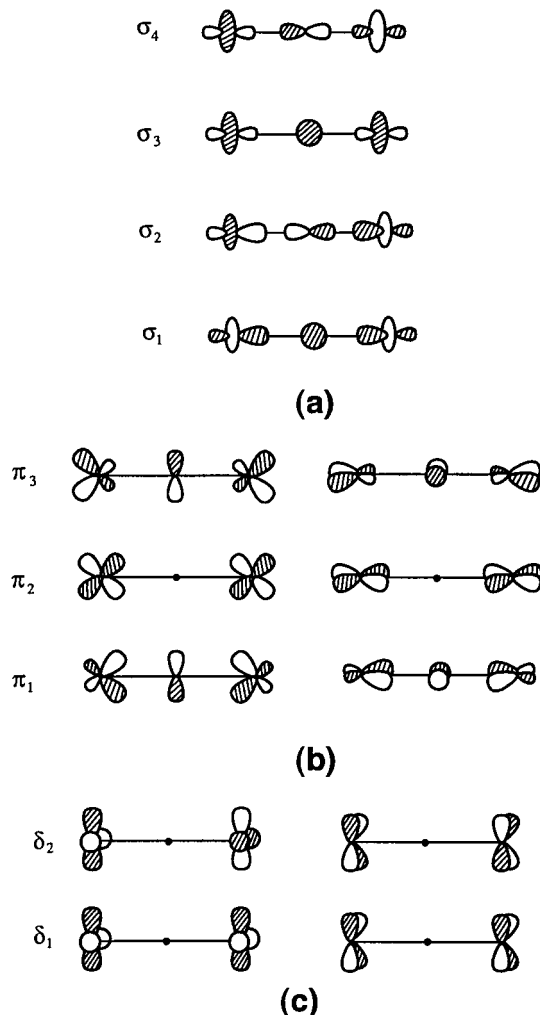


Figure 4. Molecular orbitals of the linear M–C–M units. (a) σ orbitals. (b) π orbitals. (c) δ orbitals.

Table 2. Overlap Populations of the M–C Bonds in the M–C–M Units of $\text{R}_2\text{M}_2\text{Si}_2\text{C}$ ($\text{M} = \text{Fe}, \text{Re}$), $\text{R}_2\text{Cr}_2\text{C}_3$, and RFe_2SiC as a Function of the Number of Valence Electrons *N* in the M–C–M Unit

<i>N</i>	$\text{Tm}_2\text{Fe}_2\text{Si}_2\text{C}$	$\text{Th}_2\text{Re}_2\text{Si}_2\text{C}$	$\text{Ho}_2\text{Cr}_2\text{C}_3$	ThFe_2SiC
20	0.73	1.02	0.77	0.90
22	0.73	1.02	0.76	0.90
24	0.84	1.06	0.88	0.91
28	0.73	0.99	0.76	0.82

Electronic Structures of $\text{R}_2\text{M}_2\text{X}_2\text{C}$ and RM_2XC

We calculated the electronic structures of $\text{Tm}_2\text{Fe}_2\text{Si}_2\text{C}$, $\text{Th}_2\text{Re}_2\text{Si}_2\text{C}$, $\text{Ho}_2\text{Cr}_2\text{C}_3$, and ThFe_2SiC using their $(\text{Fe}_2\text{Si}_2\text{C})^{6-}$, $(\text{Re}_2\text{Si}_2\text{C})^{8-}$, $(\text{Cr}_2\text{C}_3)^{6-}$, and $(\text{Fe}_2\text{SiC})^{4-}$ lattices, respectively. The plots of the total density of states (TDOS), the projected density of states (PDOS), and the crystal orbital overlap populations (COOP) calculated for $\text{Tm}_2\text{Fe}_2\text{Si}_2\text{C}$, $\text{Th}_2\text{Re}_2\text{Si}_2\text{C}$, $\text{Ho}_2\text{Cr}_2\text{C}_3$, and ThFe_2SiC are summarized in Figures 5–8, respectively. The overlap populations calculated for the M–C, M–X, $\text{X}\cdots\text{X}$, and $\text{M}\cdots\text{M}$ bonds of these compounds are summarized in Table 3. It is noted that the overlap populations of the $\text{M}\cdots\text{M}$ contacts are very small, although the short $\text{M}\cdots\text{M}$ distances indicate a relatively strong bonding. This is so because overlap integrals between metal d orbitals are very small.

Figure 5a shows that all the d-block levels of $\text{Tm}_2\text{Fe}_2\text{Si}_2\text{C}$ lie well below the Fermi level and hence are completely filled.

(22) Nugent, W. A.; Mayer, J. M., In *Metal–Ligand Multiple Bonds*; Wiley: New York, 1988. Section 5.4.

Table 3. Overlap Populations and Lengths (in Å) of Some Selected Bonds in $R_2M_2X_2C$ and RM_2XC Systems

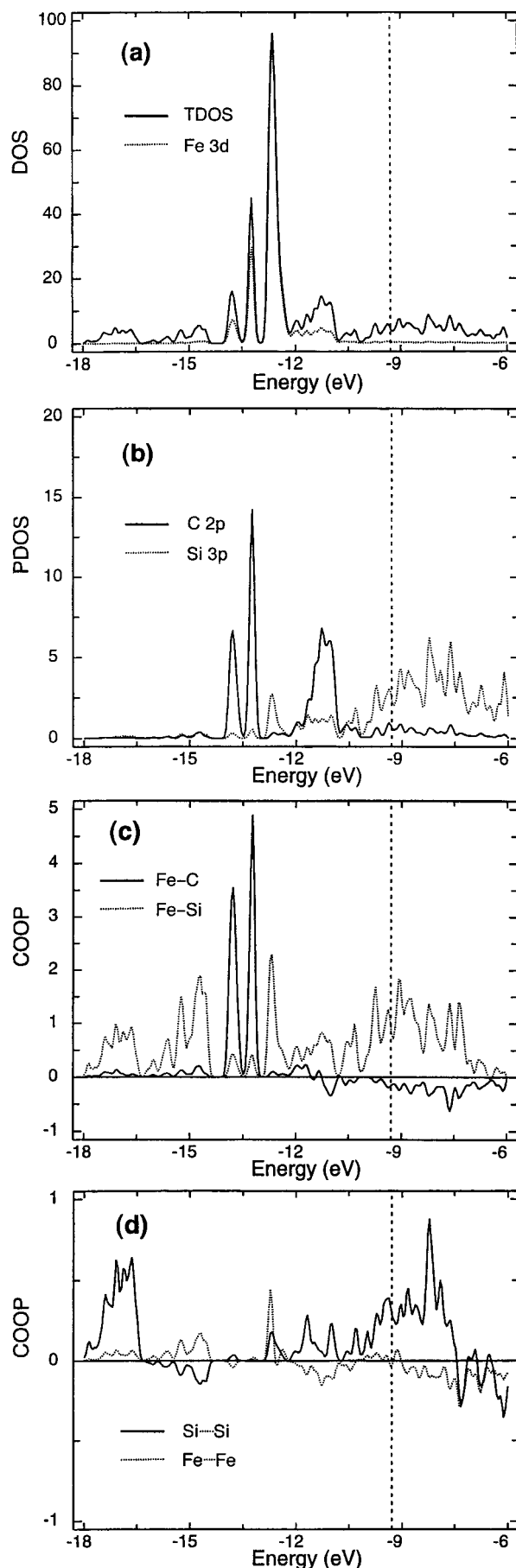
bond	$Tm_2Fe_2Si_2C$	$Th_2Re_2Si_2C$	$Ho_2Cr_2C_3$	$ThFe_2SiC$
$M-C^a$	0.78	0.78	0.88	0.81
	1.802	1.956	1.906	1.842
$M-X^{a,b}$	0.40	0.59	0.57	0.22
	2.293($\times 2$)	2.453($\times 2$)	1.984($\times 2$)	2.430($\times 2$)
	2.340	2.484	2.033	2.447
$X\cdots X^a$	0.44	0.39	0.00	
	2.591	2.741	3.604	
$M\cdots M^{a,b}$	0.04	0.12	0.02	0.06
	2.836	3.001	2.637	2.625
				2.786($\times 2$)

^a The overlap populations are given in the first row, and the bond lengths are listed in the next row(s). ^b When several bond lengths are listed, the overlap population refers to an average value.

Thus, as in the case of the phosphosilicides MSi_mP_n ,^{11,12} the d-electron count for $R_2Fe_2Si_2C$ is close to d^{10} . Figure 5b reveals that the C 2p contribution occurs primarily below the Fermi level and the Si 3p orbital contribution primarily above the Fermi level. This supports the ionic description C^{4-} , but not Si^{4-} . The PDOS plots for the C 2p and the Fe 3d orbitals have two sharp peaks around -13.5 eV. The lower and upper peaks are related to the σ_2 and π_1 levels of the Fe-C-Fe unit, respectively. The broad PDOS peak of the C 2p orbitals between -12 and -10 eV is associated with the σ_3 , σ_4 , and π_3 levels of the Fe-C-Fe unit. The COOP plot of the Fe-C bond exhibits two sharp bonding peaks around -13.5 eV (Figure 5c), which are related to the σ_2 and the π_1 levels, respectively. The COOP plot for the Fe-Si bonds shows bonding character even in the energy levels lying above the Fermi level. This, together with the PDOS plot of the Si 3p levels in Figure 5b, reveals that the Si 3p levels act as acceptor levels to the Fe 3d orbitals.^{11,12,19} Figure 5d shows that except for the narrow energy region around -15 eV, all the occupied energy levels are bonding in the Si \cdots Si bonds. Indeed, Table 3 confirms that the Si \cdots Si bond has a substantial bonding character.

The comparison of Figures 5 and 6 shows that the electronic structure of $Th_2Re_2Si_2C$ is similar to that of $Tm_2Fe_2Si_2C$. In essence, almost all the d-block levels of Re are occupied and lie below the Fermi level (Figure 6a). To a first approximation, the d-electron count for Re is close to d^{10} . Compared with the case of $Tm_2Fe_2Si_2C$, the d-orbital contributions are spread in a wider energy region and so are the top 13 MO levels of the Re-C-Re unit (Figure 3b). The PDOS peaks related to the σ_2 and π_1 levels of the Re-C-Re unit (Figure 6a,b) lie about 1 eV lower than the corresponding peaks of $Tm_2Fe_2Si_2C$, as also found for the MOs of the M-C-M units (Figure 3a,b). The C 2p orbital contribution is strong in the energy regions of the σ_2 and π_1 levels (Figure 6b) and lies mostly below the Fermi level. However, compared with the case of $Tm_2Fe_2Si_2C$, a somewhat stronger C 2p orbital contribution is present above the Fermi level in $Th_2Re_2Si_2C$ (Figure 6b). The Re-C bond is strongly bonding in the energy regions of the σ_2 and π_1 levels (Figure 6c), and it becomes antibonding in the region of the Fermi level. The Si \cdots Si bond is bonding in nearly all the occupied energy levels and immediately above the Fermi level (Figure 6d), as in the case of $Tm_2Fe_2Si_2C$. Table 3 shows that the Si \cdots Si bond has a substantial bonding character. The Re \cdots Re and Re-Si bonds of $Th_2Re_2Si_2C$ have considerably greater overlap populations than do the Fe \cdots Fe and Fe-Si bonds of $Tm_2Fe_2Si_2C$.

$Ho_2Cr_2C_3$ has two nonequivalent carbon atoms, C(1) and C(2). The C(1) atoms form the linear Cr-C-Cr units, while the C(2) atoms correspond to the Si atoms of the silicide carbides $R_2M_2Si_2C$ (M = Fe, Re). Figure 7 shows that the electronic

**Figure 5.** TDOS, PDOS, and COOP plots calculated for $Tm_2Fe_2Si_2C$. The units are in electrons per unit cell.

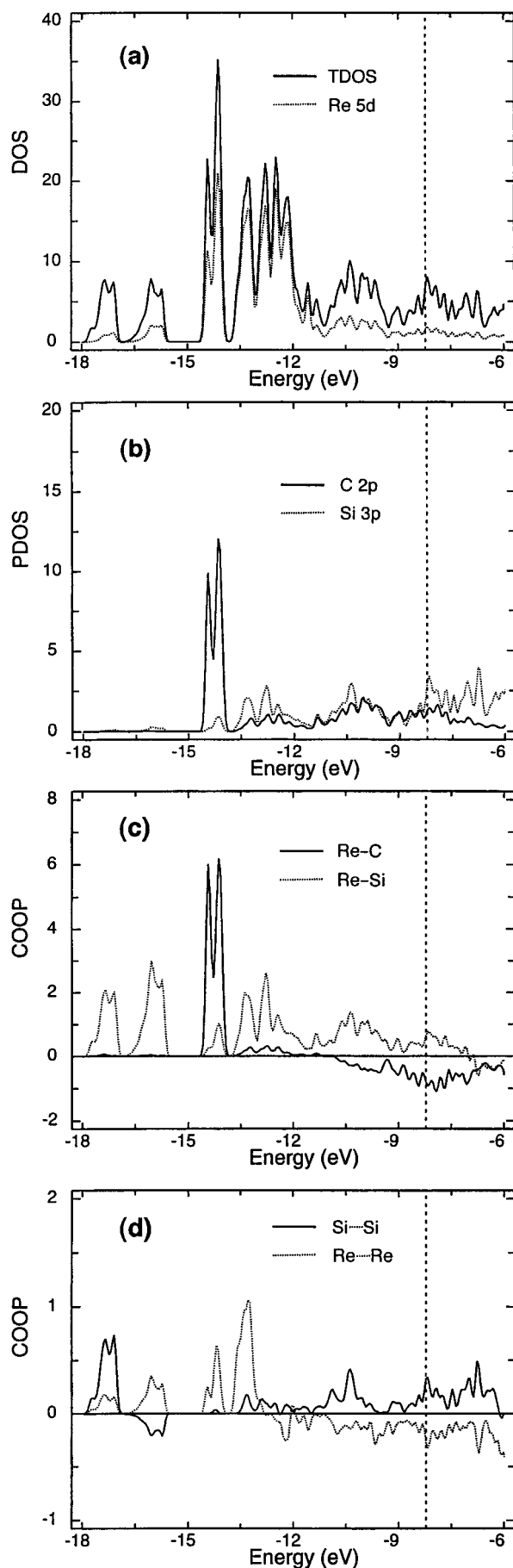


Figure 6. TDOS, PDOS, and COOP plots calculated for $\text{Th}_2\text{Re}_2\text{Si}_2\text{C}$. The units are in electrons per unit cell.

structure of the carbide $\text{Ho}_2\text{Cr}_2\text{C}_3$ is quite different than those of the silicide carbides $\text{Tm}_2\text{Fe}_2\text{Si}_2\text{C}$ and $\text{Th}_2\text{Re}_2\text{Si}_2\text{C}$. Nearly half the d-block levels of $\text{Ho}_2\text{Cr}_2\text{C}_3$ are empty (Figure 7a), and nearly a third of the C 2p levels is empty for both C(1) and C(2) (Figure 7b). The Cr–C(1) and Cr–C(2) bonds are strongly antibonding above the Fermi level (Figure 7c). The C(2)···C(2) contact shows antibonding character in the energy region well below the Fermi level and so does the Cr···Cr bond (Figure 7d). Table 3 shows that there is no bonding in the C(2)···C(2) contact, as expected from its long distance (i.e., 3.60 Å).

The electronic structure of ThFe_2SiC has many features common to those found for $\text{Tm}_2\text{Fe}_2\text{Si}_2\text{C}$. A notable difference between the two is that whereas almost all Fe 3d and C 2p orbital contributions lie below the Fermi level in $\text{Tm}_2\text{Fe}_2\text{Si}_2\text{C}$ (Figure 5a,b), small Fe 3d and C 2p orbital contributions occur above the Fermi level in ThFe_2SiC (Figure 8a,b). The latter is due to the fact that the energy levels associated with the high-lying orbitals of the Fe–C–Fe unit (e.g., σ_3 , σ_4 , and π_3) are not completely occupied. This in turn reflects that ThFe_2SiC has one less acceptor atom (i.e., Si) per Fe–C–Fe unit than does $\text{Tm}_2\text{Fe}_2\text{Si}_2\text{C}$.

Discussion

The electronic structures of $\text{Tm}_2\text{Fe}_2\text{Si}_2\text{C}$ and $\text{Th}_2\text{Re}_2\text{Si}_2\text{C}$ show that to a first approximation, the 14 MO levels of each M–C–M (M = Fe, Re) unit are completely occupied. From the viewpoint of ionic electron counting, each M–C–M unit can be regarded as an $(\text{M–C–M})^{n-}$ anion ($n = 8$ for Fe, and 10 for Re) consisting of three closed-shell ions, i.e., one C^{4-} and two d^{10} metal ions. Nevertheless, the M–C bonds of the $(\text{M–C–M})^{n-}$ anions possess a double bond character because the $(n + 1)$ s/p orbitals of M not only enhance the bonding interaction but also reduce the antibonding interaction between the nd orbitals of M and the C 2s/2p orbitals. The presence of the $(\text{M–C–M})^{n-}$ anions in the silicide carbides $\text{Tm}_2\text{Fe}_2\text{Si}_2\text{C}$ and $\text{Th}_2\text{Re}_2\text{Si}_2\text{C}$ is possible because the Si 3p orbitals lie above and hence act as acceptor levels to the 14 filled MOs of the $(\text{M–C–M})^{n-}$ anions. In terms of the $(\text{Fe–C–Fe})^{8-}$ and $(\text{Re–C–Re})^{10-}$ anions, the charge balances for $\text{Tm}_2\text{Fe}_2\text{Si}_2\text{C}$ and $\text{Th}_2\text{Re}_2\text{Si}_2\text{C}$ are given by $(\text{Tm}^{3+})_2(\text{Fe–C–Fe})^{8-}(\text{Si}^+)_2$ and $(\text{Th}^{4+})_2(\text{Re–C–Re})^{10-}(\text{Si}^+)_2$, respectively. The formal charge +1 on silicon in this electron counting is consistent with the observations that the Si 3p orbitals act as acceptor orbitals and that the Si 3p contribution to the filled energy levels is weak.

If ThFe_2SiC is assumed to have the $(\text{Fe–C–Fe})^{8-}$ anion, its charge balance is written as $(\text{Th}^{4+})(\text{Fe–C–Fe})^{8-}(\text{Si}^{4+})$. However, if the acceptor strength of Si in ThFe_2SiC is assumed to be similar to that in $\text{Tm}_2\text{Fe}_2\text{Si}_2\text{C}$, then the charge balance of ThFe_2SiC can be given by $(\text{Th}^{4+})(\text{Fe–C–Fe})^{5-}(\text{Si}^+)$. The latter implies that the top portion of the 14 MO levels of the Fe–C–Fe unit is empty. This is consistent with the electronic structure of ThFe_2SiC .

The C 2p level lies lower than the top 10 levels of the Cr–C–Cr unit (Figure 3d). Thus the C(2) atoms of $\text{Ho}_2\text{Cr}_2\text{C}_3$ cannot act as an acceptor to the Cr–C–Cr units.¹⁹ Consequently, the 14 MO levels of the Cr–C–Cr unit cannot be populated as strongly as are those of the M–C–M (M = Fe, Re) units in the silicide carbides. For the electron counting of $\text{Ho}_2\text{Cr}_2\text{C}_3$, it is convenient to rewrite its formula as $\text{Ho}_2(\text{Cr–C–Cr})\text{C}_2$. If the usual oxidation state C^{4-} for carbon is adopted for the C(2) atoms, the charge balance of $\text{Ho}_2(\text{Cr–C–Cr})\text{C}_2$ is written as $(\text{Ho}^{3+})_2(\text{Cr–C–Cr})^{2+}(\text{C}^{4-})_2$. The charge balance on the $(\text{Cr–C–Cr})^{2+}$ unit indicates that half the 14 MOs of the Cr–C–Cr unit are unoccupied. As shown in Figure 7b, the C(1) and C(2)

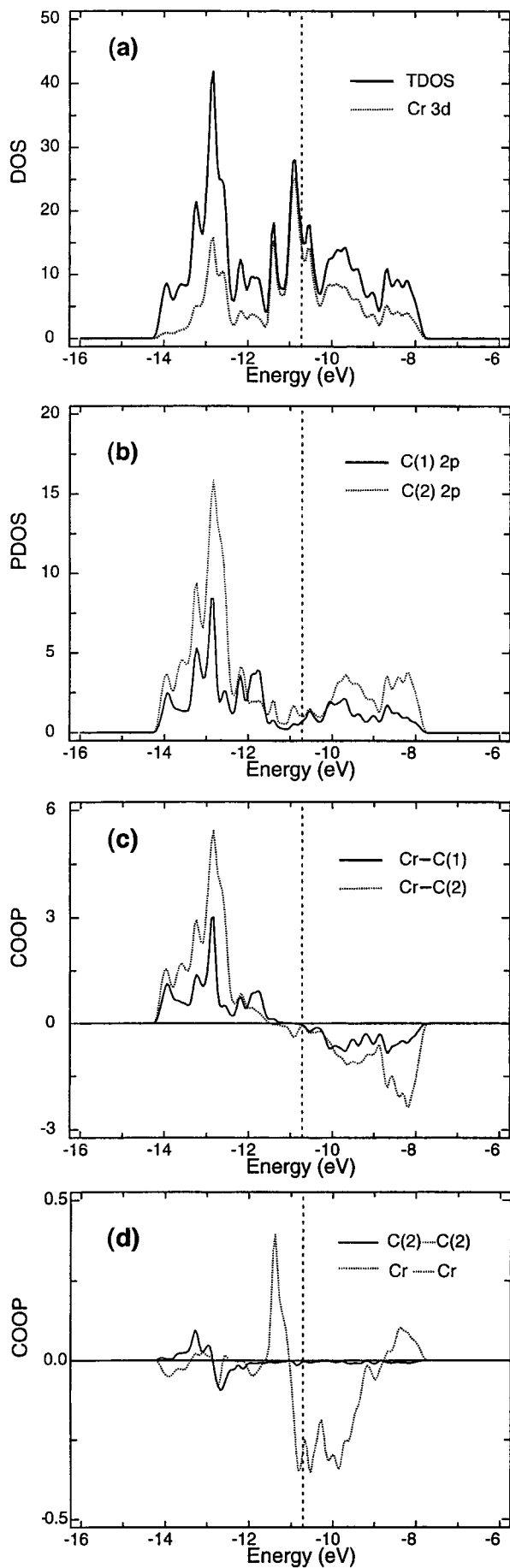


Figure 7. TDOS, PDOS, and COOP plots calculated for $\text{Ho}_2\text{Cr}_2\text{C}_3$. The units are in electrons per unit cell.

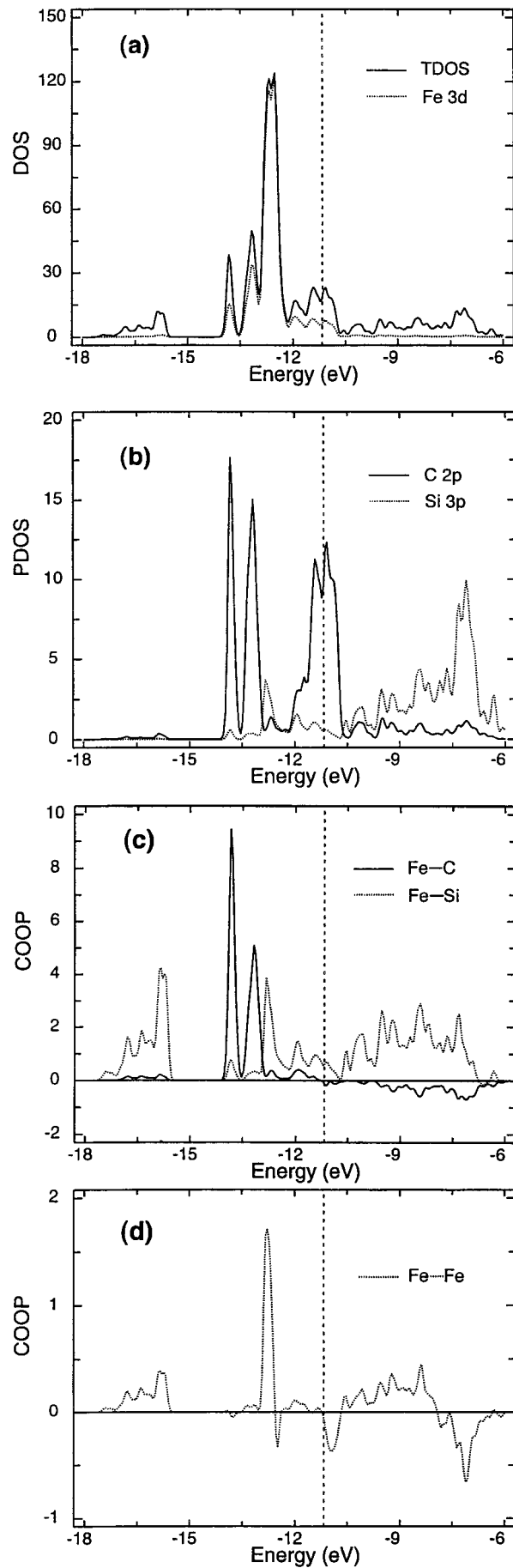


Figure 8. TDOS, PDOS, and COOP plots calculated for ThFe_2SiC . The units are in electrons per unit cell.

atoms both have a substantial amount of their C 2p contributions above the Fermi level. If the formal charge C^{3-} is used for the C(1) and C(2) atoms, then the charge balance of $Ho_2Cr_2C_3$ becomes $(Ho^{3+})_2(Cr^{1.5+})_2(C^{3-})_3$, thereby giving rise to the d-electron count $d^{4.5}$ for Cr. This picture is consistent with our finding that nearly half the d-block levels are unoccupied in $Ho_2Cr_2C_3$ (Figure 7a).

In the silicide carbides $R_2M_2Si_2C$ ($M = Fe, Re$), the interlayer $Si \cdots Si$ distances are significantly shorter than the van der Waals distance. The p-block levels of the Si atoms are nearly empty in the silicide carbides so that the formation of the short $Si \cdots Si$ contacts in $R_2M_2Si_2C$ manifests the tendency for electron deficient centers to aggregate together.²³ In contrast, the interlayer $C(2) \cdots C(2)$ distances in the carbides $R_2Cr_2C_3$ are longer than the van der Waals distance. The p-block levels of the C(2) atoms are almost completely filled in the carbides $R_2Cr_2C_3$, so that the occurrence of the long $C(2) \cdots C(2)$ contacts in $R_2Cr_2C_3$ reflects the tendency for electron-rich centers to stay far apart.²³

Let us now examine the electronic structures of $Tm_2Fe_2Si_2C$, $Th_2Re_2Si_2C$, and $ThFe_2SiC$ from the viewpoint of the modified electron counting (MEC) scheme proposed recently.^{11,12} To a first approximation, the interlayer $Si \cdots Si$ bond of $Tm_2Fe_2Si_2C$ may be treated as a single bond since its overlap population is substantial. Then, according to the conventional electron counting (CEC) scheme, in which the electron pair of a metal–ligand bond is counted as the lone pair belonging to the ligand atom, the formal charges on the main group units are given by $(Si-Si)^{6-}$ and C^{4-} . Therefore, the charge balance of $Tm_2Fe_2Si_2C$ is written as $(Tm^{3+})_2(Fe^{2+})_2(Si-Si)^{6-}(C^{4-})$. The formal charge Fe^{2+} implies that two d-block levels per Fe are empty, and the $(Si-Si)^{6-}$ anion implies that its six lone pair levels are completely filled. The Si lone pair level lies higher than the Fe d-block level.²¹ Thus, according to the MEC scheme,^{11,12} eight electrons should be transferred from the $(Si-Si)^{6-}$ anion to fill the four empty d-block levels of the two Fe^{2+} cations per formula unit. This leads to the charge balance $(Tm^{3+})_2(Fe^{2-})_2(Si-Si)^{2+}(C^{4-})$ for $Tm_2Fe_2Si_2C$, which is equivalent to the $(Tm^{3+})_2(Fe-C-Fe)^{8-}(Si^+)_2$ picture discussed above. The $(Si-Si)^{2+}$ ion has six lone pair levels with four electrons in them. Thus, the MEC scheme predicts that the frontier orbitals of $Tm_2Fe_2Si_2C$ are given by the Si lone pair levels, in agreement with the electronic structure of $Tm_2Fe_2Si_2C$. In a similar manner,

the charge balance for $Th_2Re_2Si_2C$ can be written as $(Th^{4+})_2(Re^+)_2(Si-Si)^{6-}(C^{4-})$, according to the CEC scheme and as $(Th^{4+})_2(Re^{3-})_2(Si-Si)^{2+}(C^{4-})$, according to the MEC scheme. The charge balance for $ThFe_2SiC$ is written as $(Th^{4+})(Fe^{2+})_2(Si^{4-})(C^{4-})$, according to the CEC scheme. The Si 3p level lies higher, but Si 3s level lies lower, than the Fe 3d level.²² Therefore, the Si^{4-} ion has only six electrons available for electron transfer to fill the four empty d-block levels of two Fe^{2+} ions. Thus, the charge balance for $ThFe_2SiC$ is given by $(Th^{4+})(Fe^-)_2(Si^{2+})(C^{4-})$, according to the MEC scheme. From the viewpoint of the Fe–C–Fe unit, this picture implies $(Fe-C-Fe)^{6-}$. The latter in turn means that one of the doubly degenerate p_3 level of the Fe–C–Fe unit is empty. This picture is consistent with the electronic structure of $ThFe_2SiC$ described above.

Concluding Remarks

Our study shows that the M–C bonds of the discrete linear M–C–M ($M = Cr, Fe, Re$) units in the compounds $R_2Fe_2Si_2C$, $R_2Re_2Si_2C$, RFe_2SiC , and $R_2Cr_2C_3$ should be regarded as double bonds. This supports the double-bond description given by Jeitschko and co-workers^{6,7} for the Fe–C and Re–C bonds of $R_2Fe_2Si_2C$ and $R_2Re_2Si_2C$. The 14 MOs of the linear M–C–M units in $R_2Fe_2Si_2C$ and $R_2Re_2Si_2C$ are completely filled because the Si 3p levels act as acceptor levels to these MOs. This leads to the d^{10} electron count for the Fe and Re atoms. The same conclusion is reached by using the MEC scheme. The electrons around the Fermi level of these compounds have largely the character of the Si 3p orbitals. The d-electron count for the Fe atoms of $ThFe_2SiC$ is slightly lower than d^{10} , because $ThFe_2SiC$ has one less acceptor atom (i.e., Si) per Fe–C–Fe unit than does $Tm_2Fe_2Si_2C$. The interlayer $Si \cdots Si$ distances of the silicide carbides $R_2M_2Si_2C$ ($M = Fe, Re$) are significantly shorter than the van der Waals distance because the p-block levels of the Si atoms are nearly empty. The interlayer $C \cdots C$ distances of the carbides $R_2Cr_2C_3$ are longer than the van der Waals distance because the p-block levels of the carbon atoms are almost completely filled.

Acknowledgment. The work at North Carolina State University was supported by the Office of Basic Energy Sciences, Division of Materials Sciences, U.S. Department of Energy, under Grant DE-FG05-86ER45259. M.-H.W. thanks Professor W. Jeitschko for reprints of his work.

IC981309A

(23) Reference 19, Chapter 7.